Experimental and Theoretical Research on Liquid Entrainment in AP1000 ADS Blow-down Phase of SBLOCA

S.Z. Qiu*, D.C. Sun, W.X. Tian, Y. Xiang, G.H. Su
School of Nuclear Science and Technology, Xi'an Jiao Tong University
28 Xianning West Road, Xi'an 710049, China
szqiu@mail.xjtu.edu.cn; duchengsun@stu.xjtu.edu.cn; wxtian@mail.xjtu.edu.cn

P. Zhang
State Nuclear Power Technology R&D Center
Beijing, 100190, China
zhangpeng5@snptc.com.cn

ABSTRACT

The fourth stage Automatic Depressurization System (ADS-4) enables controlled depressurization of reactor coolant system during small break LOCA. However, the coolant may be entrained into the containment through the ADS-4 branch line simultaneously, which reduces the coolant inventory in the primary loop and poses great threats to reactor core uncovering and melting.

To make up for the deficiency of liquid entrainment database in advanced passive safety PWR, the Automatic Depressurization and Entrainment TEst Loop (ADETEL) modeled after AP1000 with a scaling ratio 1:5.6 was constructed, and the test data of ADS-4 entrainment and upper plenum entrainment were collected and analyzed. The experiments were conducted at atmospheric pressure with the maximum steam flow rate of 700kg/h. The entrainment processes were recorded by a high speed camera and interesting details were captured.

A clear difference exists between ADETEL ADS-4 entrainment onset data and available correlations, which may caused by the differences in fluids physical properties, horizontal pipe flow conditions, determination methods of entrainment onset and geometries (e.g., diameter ratio between branch and hot leg, d/D). The upper plenum entrainment test data shows that the entrainment deposition effect of the reactor internals is smaller than the entrainment promotion effect due to the decrease of flow area and acceleration of steam in the upper plenum. Using the visualization information gained from experiments, the authors develop a model for predicting the entrainment onset in upward tee branch. The model is compared against the experimental data and shows good agreement.

KEYWORDS
AP1000, ADS-4 entrainment, Upper plenum entrainment, ADETEL, Model

1. INTRODUCTION

The fourth stage Automatic Depressurization System (ADS-4) is an important part of the passive safety feature in Westinghouse AP1000 design which provides a controlled depressurization during the small break LOCA. ADS-4 valves are connected to the hot legs and discharge directly to the containment atmosphere and therefore system depressurization is achieved. When the Core Makeup Tank (CMT) level

* E-mail address: szqiu@mail.xjtu.edu.cn (S.Z. Qiu).

drops to 20%, the ADS-4 valves are activated automatically and depressurize the Reactor Coolant System (RCS) to 89.6kPa higher than the containment pressure [1]. Then the gravity injection of the In-Containment Refueling Water Storage Tank (IRWST) is established, which marks the end of the small break LOCA transient and the beginning of the long-term cooling [2]. However, the coolant in the hot leg may be carried into the containment through the ADS-4 branch line by the flowing steam, as illustrated in Figure. 1. The phenomenon is defined as liquid entrainment and leads to coolant inventory loss, which poses great threat to core uncovering and melting.

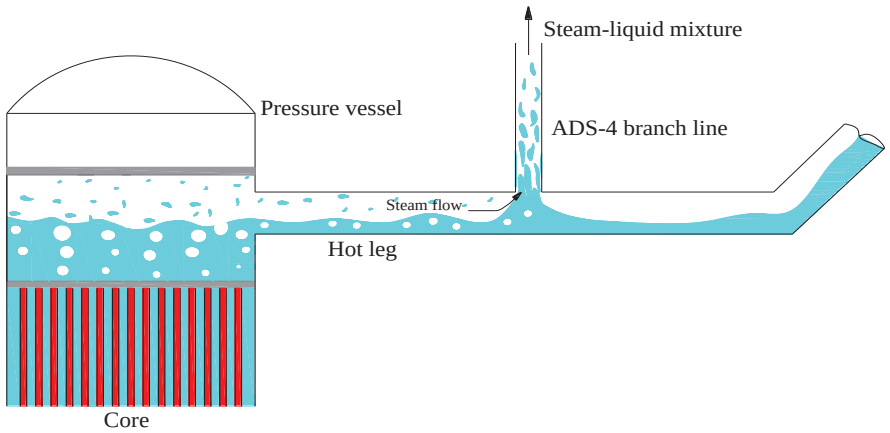

Figure 1. ADS-4 depressurization and entrainment process in AP1000. [3]

ADS-4 adopts reduced tee branch to realize the phase separation process. When the critical liquid level in the horizontal main line is reached under certain gas flow rate, the pressure difference generated at the reduced tee branch may overcome the suppression effect of the surface tension and gravity, and liquid drops or columns begin to separate from the gas-liquid interface. This is defined as the onset of liquid entrainment (OLE).

The upper plenum entrainment is a kind of pool entrainment with a horizontal side branch, as illustrated schematically in Fig. 2. Liquid drops or columns from the upper plenum are entrained by the steam, pass through the reactor internals and enter the hot leg. Some of the liquid drops or columns can be carried to the containment directly through the ADS-4 branch line. The upper plenum entrainment can further reduce the coolant inventory in the reactor primary loop.

Zuber [5] indicated that liquid entrainment through small break may occur in LOCA. Since then, the vertical up tee branch entrainment with various geometries and working fluids have been investigated by many researchers. Smoglie [6] developed the OLE and entrainment rate models based on their experimental data and the OLE model was adopted by RELAP5 MOD3.2 version [7]. Schrock et al. [8] conducted the upward tee branch entrainment experiments with air-water and steam-water. OLE and entrainment rate experiments were conducted with four branch inner diameters ranging from 3.76 mm to 10.15 mm. OLE and entrainment rate models were developed by fitting the experimental data. Steam-water was used as the working fluids in Maciaszek et al.' [9] entrainment experiment. The OLE model was developed based on the interface instability. The semi-empirical entrainment rate model was developed by fitting the experimental data.

ATLATS was a separate effect test facility scaled after AP600 to investigate the ADS-4 entrainment phenomenon. The OLE and entrainment rate experiments were conducted with air-water by Welter et al.

[10]. Wave theory was introduced in the development of entrainment models. AP1000 has a larger ADS-4 d/D (~0.58) ratio than AP600 (~0.33), and therefore the ATLATS test data may not reflect the entrainment process in ADS-4 for AP1000.

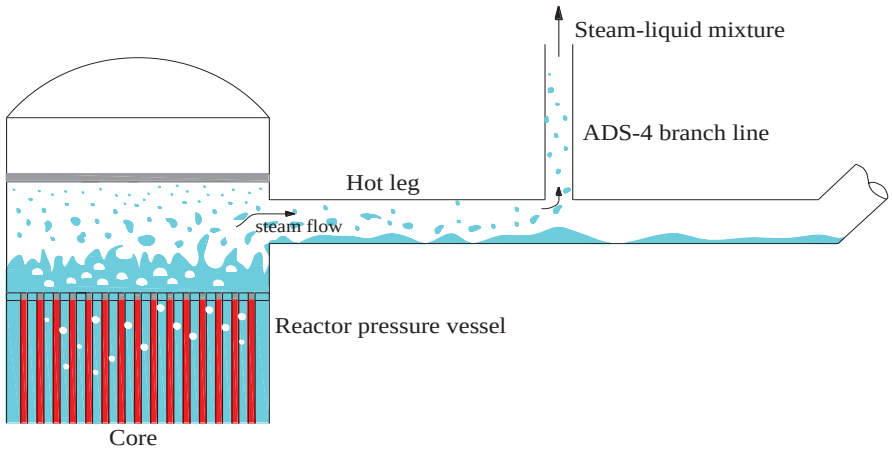

Figure 2. Upper plenum entrainment process in AP1000. [4]

Sun et al [11] conducted the visualization experiments with double-end gas inlets to investigate the ADS-4 tee branch entrainment phenomena in AP1000. Besides the entrainment onset and entrainment rate tests, the entrainment frequency was also studied. The test data reveal that the entrainment period decreases rapidly with the increase of entrainment rate in low range of the entrainment rate, and gradually stabilizes in high range of the entrainment rate.

ADS-4 blow down and depressurization experiments were also conducted in integrated facilities, such as APEX and SPES. However, integrated behaviors under accident conditions were emphasized in the experiments while less attention was paid on ADS-4 branch entrainment [1].

A correlation was developed for the pool entrainment amount based on simple mechanistic modeling and a number of test data by Kataoka et al. [12]. Three regions of entrainment in the axial direction from a pool surface were proposed, namely the near surface region, momentum controlled region and deposition region. The correlation agrees well with a large number of experimental data over a wide range of pressure for air-water and steam-water systems.

Experimental study of liquid entrainment and off-take from the swelled two-phase mixture surface in a vessel was conducted by Kim et al. [13]. A total of 220 experimental data on the entrainment and off-take were obtained using a test vessel with an inner diameter of 0.3m and a top break with a diameter of 0.05m.The upper plenum entrainment transient experiment was conducted by Wu et al. [14] with air-water. The study was undertaken on the modified ATLATS facility which scaled after Westinghouse AP1000. The deposition effect of reactor internals was taken into consideration. Test results showed that the pool entrainment correlations developed by Kataoka et al. [12] deviated largely from the test data and therefore the in-vessel liquid entrainment phenomena were not likely pool entrainment.

It is seen from the review that the flow conditions, test section geometries and physical properties deviate greatly from those in the prototypical conditions. Besides, existing entrainment models adopted by known system codes (TRACE, RELAP5) underestimate the ADS-4 entrainment amount. In the series 25 of APEX data, core uncovering was experienced, while RELAP5 simulations revealed a completely

submerged core [15]. Furthermore, upper plenum entrainment was not considered in known codes like TRACE and RELAP5 [14]. Further experimental investigations are needed to develop general models or modify the established models. Therefore, the Automatic Depressurization and Entrainment TEst Loop (ADETEL) was constructed to cover the shortage of entrainment database and gain more insights into the entrainment phenomena in AP1000 ADS blow-down phase of SBLOCA. The experiment and ADS-4 entrainment onset modeling will be introduced in the following chapters.

2. ADETEL test facility

The ADETEL test facility located in Xi'an Jiaotong University is modeled after AP1000 based on a scaling analysis. The upper plenum entrainment process during the actuation of ADS-4 and the onset of gravity injection of IRWST (In-Containment Refueling Water Storage Tank) can be investigated on ADETEL. A comprehensive scaling analysis was conducted and a set of scaling ratios were obtained to preserve the prototypical conditions [16]. The scaling ratios of hot leg diameter and height were chosen as 1:5.6 and other geometric and thermal hydraulic parameter ratios between ADETEL and AP1000 were obtained based on the scaling analysis described in reference [16]. The ADETEL facility for entrainment studies is shown schematically in Figure 3. Air-water and steam-water can be employed as the working fluids. The experiments were conducted under atmospheric conditions. In steam-water experiment introduced in this paper, electrically heated rods with the maximum 450 kW are used to simulate the decay heat of the reactor. The maximum steam flow rate is about 700kg/h. The deionized water is stored and preheated in the heating tank with a volume of 3.0m^3. A high-temperature pump with a capacity of 15t/h is used to deliver the water to the pressure vessel. The water will be preheated again by a preheater with a capacity of 180kW before entering the pressure vessel. The saturation temperature of water can be reached at the inlet of pressure vessel. This can be achieved by regulating the heating power of the preheater automatically or manually through a control panel. The power in the pressure vessel is utilized to provide the latent heat of vaporization.

The pressure vessel is made of austenitic stainless steel with an inner diameter about 600mm. The gas-liquid mixture flows through the hot leg and is separated in the weighing tank. The mass of the entrained water is measured by weighing transducers and the separated steam is discharged into the atmosphere. The two-phase mixture in the upper plenum flows around the 38 rod bundles (simulator of guide tubes and upper support columns) of 40 mm outer diameter, and finally exits the reactor vessel through the hot leg. For accurately simulating the experimental phenomena, half of the vessel is considered to model one of the two hot legs in AP1000.

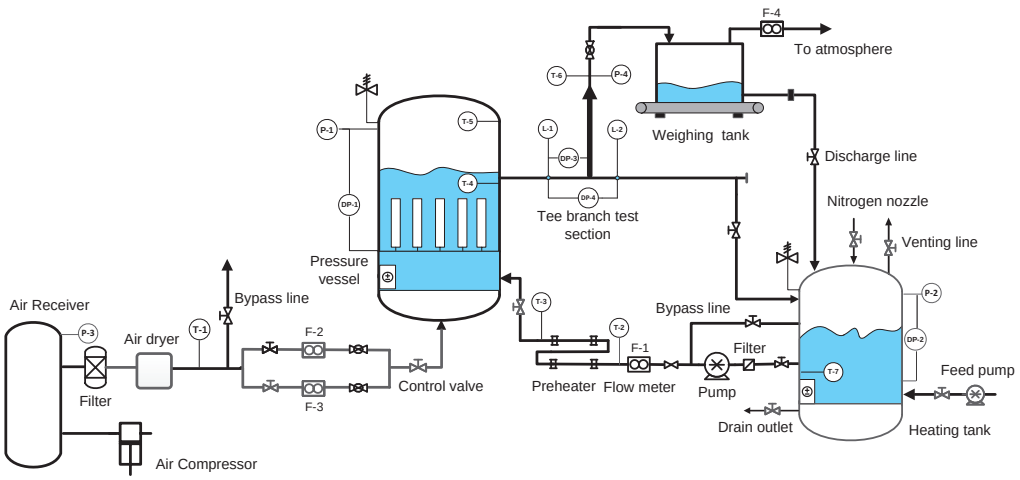

Figure 3. Schematic of ADETEL facility. [17]

The National Instruments acquisition system is used and an interface panel based on LabVIEW is programmed to collect and save test data. A control panel is used to regulate the heating power rate automatically or manually. The mixture liquid level in the pressure vessel is measured by a capacitance probe. The collapsed liquid levels in the pressure vessel and the heating tank are measured by pressure difference transducers. Thermal resistances are employed to measure the temperature in various locations. The main source of the data uncertainty in the experiment includes data measurement errors of the instrumentation and collection errors of the data acquisition system. The relationship between standard uncertainty, u(a), and instrumental errors, Δ_{ins}, can be expressed as:

$$u(a) = k \times \Delta_{ins} \tag{1}$$

Where k is the coverage factor and $\sqrt{3}$ is chosen assuming the instrumental errors obey the uniform distribution. The maximum error of the National Instruments acquisition system is 0.02%. According to the range and the maximum permissible error of the instruments, the data uncertainty of steam flow rate, liquid levels in the hot leg and pressure vessel are $\pm$0.030kg/s, 0.44mm, 2.4mm, respectively.

3. RESULTS AND DISCUSSION

3.1. ADS-4 entrainment experiment

The operation pressure was slightly higher than the atmospheric pressure. The test facility should be warmed up and the transducers should be calibrated before each group of test. The steam flow rate could be measured downstream of the weighing tank. However, the condensation in the pipeline and weighing tank could introduce large data uncertainty. Therefore the calibration was conducted by installing a V-cone flowmeter just above the ADS-4 branch to determine the thermal efficiency of the test facility (relationship between the steam flow rate and the heating power), which was 97.3%. The steam flow rate in this experiment was calculated from the heating power.

The entrainment onset can be determined by visualizing the appearance of droplets from the gas-liquid interface, and also can be judged by the rise of pressure difference signal between the branch and the hot leg. However, the above methods were not applicable in this experiment due to the liquid level fluctuations in the horizontal hot leg. Therefore, a “up to bottom” method adopted in ATLATS is used to determine the entrainment onset condition. In this method, the hot leg is filled with saturated water initially in the entrainment onset experiment. Then the power is supplied and entrainment process is established. The hot leg liquid level continues decreasing due to the liquid entrainment and vaporization until the entrainment onset liquid level is reached. A turning point exists in the hot leg liquid level curve before and after the entrainment onset condition, and the corresponding liquid level in the hot leg is treated as the entrainment onset liquid level.

In the entrainment rate experiment, steam was supplied at a specified rate and the saturation water was injected to the pressure vessel. The stabilized entrainment process is established at certain hot leg liquid level when the water injection rate is balanced by the liquid entrainment rate and vaporization rate. The vaporized steam flow rate can be calculated by the input heating power in the pressure vessel. The liquid entrainment amount is therefore the difference between the water injection rate and the steam vaporization rate. Increase the water injection rate stepwise and the entrainment will be stabilized at a higher liquid level.

Typical entrainment rate process was recorded by a high speed camera with 800fps. The entrainment occurred not continuously but with certain frequency. The typical entrainment process is presented in Fig. 4. The steam flow rate was 0.08kg/s and the liquid flow rate was 0.3kg/s. The inclined two-phase interface plane took form beneath the branch to connect the liquid level gap upstream and downstream of the branch. The water tended to accumulate and stayed downstream the branch under the action of force

generated from the flow direction change of steam. The liquid level downstream the branch kept rising and the water from the pressure side climbed the inclined plane and eventually was entrained to the branch. The slug flow could be formed downstream the branch and the reversed flow was clearly visible at the inlet of the branch as sketched with yellow lines.

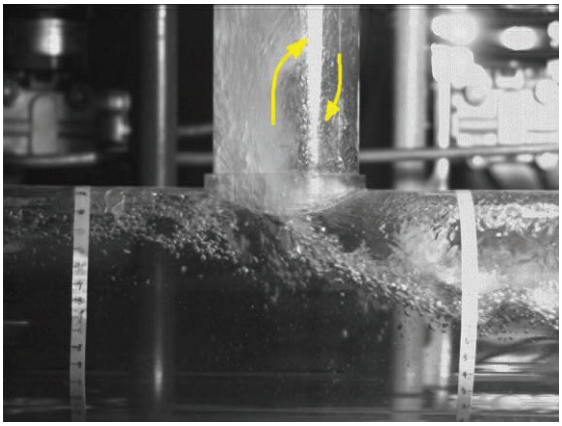

Figure 4. Tee branch entrainment process for intermittent flow

3.1.1 Entrainment onset

The entrainment onset data were collected and compared with existing experimental data and models. The comparison of experimental data with the entrainment onset models is shown in Fig. 5. The branch Froude number, Fr_d, is a dimensionless number defined as the ratio of the flow inertia to the gravity, which can be expressed as:

$$Fr_d = \frac{v_3\sqrt{\rho_g}}{\sqrt{gd\left(\rho_f - \rho_g\right)}} \tag{2}$$

It is observed that the branch steam Froude number increases with the dimensionless OLE gas chamber height, h_b/d both in models and experimental data. However, discrepancies are found between experimental data and models, which may be caused by differences in fluids physical properties, d/D ratios, the horizontal pipe flow conditions and the methods of determining the entrainment onset. The model developed by Smoglie et al. [6] is quite close with that developed by Schrock et al. [8]. The entrainment onset occurs at lower Fr_d for the same gas chamber height. The models are close with the experimental data at low h_b/d range. But the difference grows larger with the increase of h_b/d. It is worth mentioning that the correlation developed by Smoglie et al. [6] is adopted by RELAP5 MOD3.2 version [18]. Therefore, the RELAP5 code may not applicable to the ADS-4 entrainment onset estimation in AP1000, especially in the low hot leg liquid level conditions. The flow conditions in the hot leg are much alike for ATLATS and ADETEL, and similar methods of determining the entrainment onset are adopted. However, considerable difference still exists between ADETEL data and ATLATS OLE model, which may be attributed to the difference in fluids physical properties and dimensional effect introduced by different d/D ratios.

3.1.2 Entrainment rate

Entrainment rate test data were also collected under different steam flow rates. Figure 6 illustrates the relationship between branch quality, x_3, and dimensionless gas chamber height, h/D, under various steam flow rates, where x_3 is expressed as:

$$x_3 = \frac{1}{1 + w_f / w_g} \tag{3}$$

It shows that the branch quality increases with the dimensionless gas chamber height. In the low range of h/D, the branch quality grows slowly with the h/D. While the branch quality increases rapidly for large h/D. Therefore, the amount of entrained water will drop dramatically with the decreases of liquid level for lower liquid level in the hot leg at a specified steam flow rate. Similar trends are found in the 7 curves at different steam flow rates. It can be observed that the branch quality increases with the gas flow rate under the same gas chamber height.

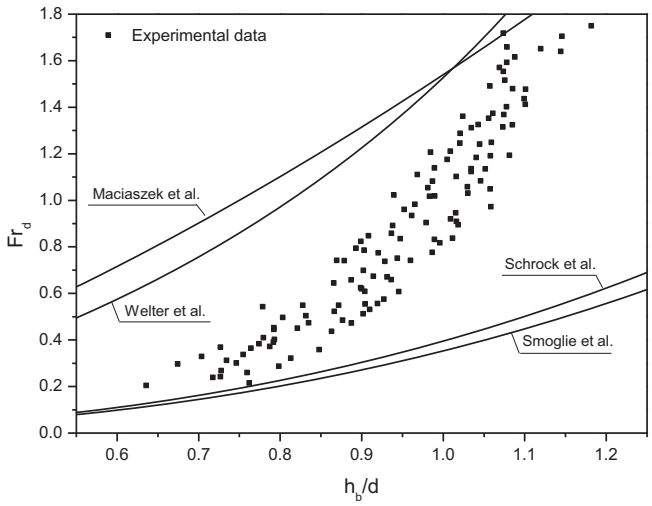

Figure 5. Comparison of experimental data with entrainment onset correlations. [3]

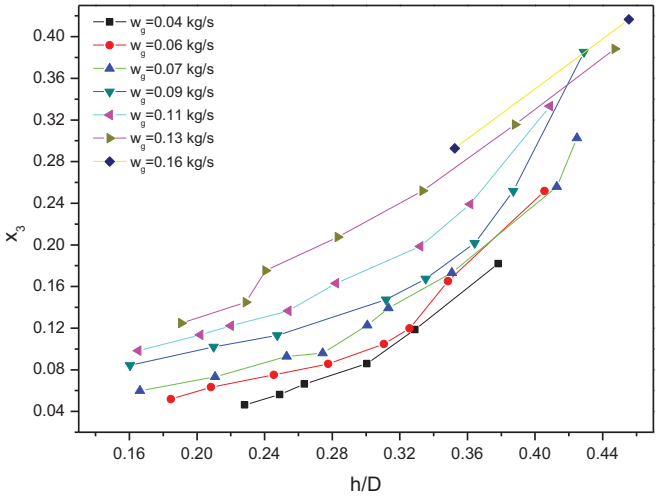

Figure 6. Comparison of entrainment rate under different steam flow rates. [3]

3.2. Upper plenum entrainment

Steady state experiments were conducted with various combinations of the mixture liquid level in the pressure vessel and the steam flow rate. The water injection rate can be balanced by the loss of water due to the vaporization and entrainment. Increase the pressure vessel heating power rate while keep the flow

injection rate constant, the mixture liquid level in the pressure vessel could decrease due to the increase of vaporization rate. The entrainment amount therefore decreased and the entrainment process eventually stabilized at a lower mixture liquid level. The steam flow rate and the instantaneous distance between the bottom of hot leg and the mixture level in the pressure vessel are two critical parameters determining the upper plenum entrainment rate. The liquid could accumulate in the hot leg due to the upper plenum entrainment. However, the liquid could not flow back into the pressure vessel due to the blocking effect of the steam as observed in the experiment.

The test data were collected and analyzed. Entrainment is expressed as the ratio of the liquid drops mass flux, $\rho_f j_f$, to the steam mass flux, $\rho_g j_g$, namely:

$$E_{fg} = \frac{\rho_f j_f}{\rho_g j_g} \tag{4}$$

The relationship between entrainment and h* under different steam flow rates without reactor internals is illustrated in Figure 7. h* is the dimensionless height between the two-phase mixture surface and the bottom of the hot leg. It is expressed as:

$$h^* = \frac{h}{\left(\frac{\sigma}{g\Delta\rho}\right)^{0.5}} \tag{5}$$

Where h is the distance between the two-phase mixture surface and the bottom of the hot leg. It can be seen that the steam flow has little effect on the entrainment under stable experimental conditions. The entrainment rate and mixture liquid level in the pressure vessel remain constant when the entrainment process is stabilized. Increase the steam flow rate by increasing the heating power and the mixture liquid level in the pressure vessel will increase accordingly. The entrainment process becomes more violent and large amount of water is entrained to the hot leg. The mixture level in the pressure vessel therefore drops and finally stabilizes at a lower level than the previous steady state level when constant water injection rate is supplied. The entrainment rate is suppressed due to the decrease of mixture liquid level. This may be the reason why entrainment rate is not sensitive to the changes of the steam flow rate under stable experimental conditions.

The h* range in current stable experiment covers the near surface region and momentum controlled region as defined in the entrainment model developed by Kataoka et al. [12]. The dimensionless height range of the two regions are listed as follows.
Near surface region:

$$0 \le h^* \le 1.038\times10^3 j_g^* N_{\mu g}^{0.5} D_H^{*0.42} \left(\frac{\rho_g}{\Delta\rho}\right)^{0.23} \tag{6}$$

Momentum controlled region:

$$1.038\times10^3 j_g^* N_{\mu g}^{0.5} D_H^{*0.42} \left(\frac{\rho_g}{\Delta\rho}\right)^{0.23} \le h^* \le 1.97\times10^3 N_{\mu g}^{0.33} D_H^{*0.42} \left(\frac{\rho_g}{\Delta\rho}\right)^{0.23} \tag{7}$$

Where $N_{\mu g}$, D_H^* are gas viscosity number and dimensionless hydraulic diameter of vessel as introduced in reference [12]. When the steam was supplied at 347kg/h, the height of near surface region situates between 0 and 6.2, and the height of momentum controlled region situates between 6.2 and 65.9. It can be seen that the entrainment in near surface region is much higher than that in the momentum controlled region. In the low range of h*, the entrainment decreases dramatically with the increase of h*. While the entrainment curves under different steam flow rates flatten out gradually in the high range of h*. It suggests that in the low range of h*, the upper plenum entrainment amount drops dramatically with the increase of h*. As the mixture liquid level in the pressure vessel decreases, both the entrainment amount and the entrainment amount decreasing rate decline. Only fine droplets can be entrained to the hot leg

when the mixture liquid level drops to a certain value and the decrease of liquid level in the pressure vessel is mainly due to the vaporization.

The comparison between the test data and the Ishii's pool entrainment model [12] is shown in Fig. 8. The steam flow rate in the experiment was large and located in the high gas flux region of the momentum controlled region as defined in Ishii's pool entrainment model [12]. However, Kataoka and Ishii [12] didn't give exact entrainment correlation in high gas flux regime. Therefore, the test data are compared only with the near surface region of the model. It can be seen from Fig. 8 that the entrainment amount in the experiment is much lower than the prediction results of the model. The huge discrepancy suggests that the upper plenum entrainment mechanism with a side branch is different from that of the pool entrainment. The near surface region comprises all the entrained droplets in Ishii's pool entrainment model [12]. However, only the droplets in the vicinity of the hot leg branch can be entrained outside of the pressure vessel due to the Bernoulli effect, and the droplets far from the hot leg branch will deposit on the gas-liquid interface again.

4. MODELING OF ADS-4 ENTRAINMENT ONSET

The ADS-4 entrainment onset process can be divided into wave formation and wave spilt. The schematic of entrainment onset is shown in Figure 9. The waves upstream and downstream of the branch is neglected in the figure for brevity. The waves in the hot leg are formed under the effect of Kelvin-Helmholtz instability. According to the Bernoulli effect, the waves in the hot leg tend to form upstream/downstream the branch rather than directly below the branch. Given the wave profile captured in the experiment, assuming the gas-liquid interface follows cosine distribution with the amplitude $a_0/2$ and wave length λ. The waves from both sides of the tee branch move toward each other and overlapped under the tee branch. The standing wave can be formed and the antinode forms directly under the tee branch in the hot leg. The amplitude distribution of the standing wave in the coordinate system can be expressed as:

$$a(x) = a\cos\left(2\pi\frac{x}{\lambda}\right) \tag{8}$$

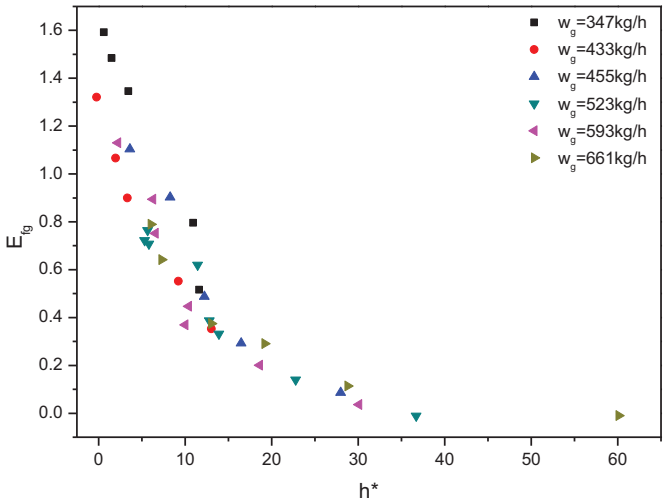

Figure 7. Relationship between entrainment and dimensionless height. [4]

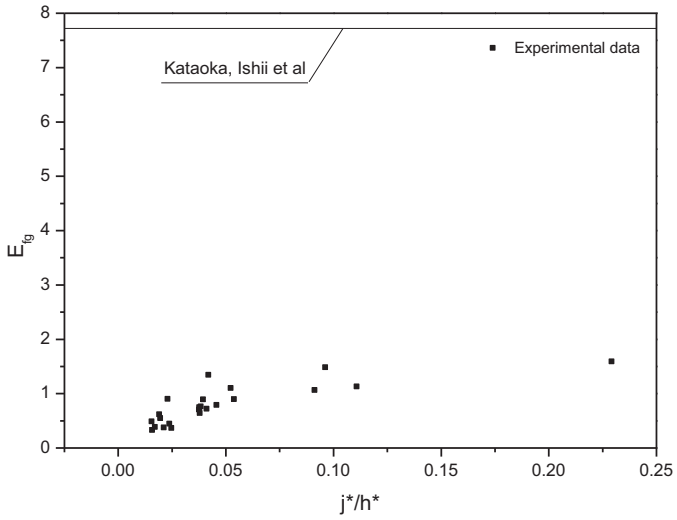

Figure 8. Comparison of test data with Ishii's pool entrainment model

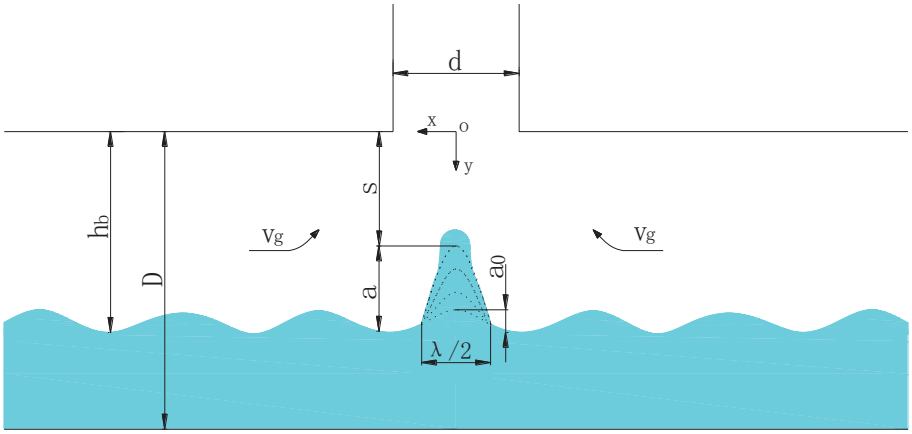

Figure 9. Schematic of entrainment onset.

The crest experiences a reduced pressure due to the Bernoulli effect and the crest keeps growing following the cosine profile. The surface tension force acts along the length of the wave crest and its vertical component opposes the suction of the steam. If the drag force acts on the wave crest is larger than the combined effect of the surface tension and gravity, the liquid column will deform into liquid drops. Before breaking into liquid drops, assuming that a liquid hemisphere is formed with the radius equal with the curvature radius of the wave crest, which can be expressed as:

$$R = \frac{\lambda^2}{4\pi^2 a} \tag{9}$$

At the entrainment onset condition, the drag force overcomes the surface tension and gravity at the wave crest and expressed as:

$$F_D \geq F_\sigma + F_g \tag{10}$$

The above equation can be calculated as:

$$\frac{1}{2} C_D \rho_g \left(u_g - u_f\right)^2 A \geq \sigma \cdot 2\pi R + \rho_f \frac{2}{3} \pi R^3 g \tag{11}$$

Where C_d is the drag coefficient and A is the wave cross section area.

By neglecting the gas viscosity under steady state conditions, potential flow theory is applicable and the gas phase field is generated by an assumed point sink located at the branch inlet. According to the conformal transformation theory [19], a point sink with the strength 2Q exists at point b in the supplementary plane (Figure 10a) corresponding to the point sink located at point B in the physical plane (Figure 10b), and the point source with the strength Q at point a exists in the supplementary plane corresponding to the parallel flow with the flow rate Q/2 from the right side of the horizontal main pipe in the physical plane. Apply singularity superposition theorem [19] and Schwarz-Christoffel transformation [19] and the flow complex potential can be obtained as:

$$F(z) = -\frac{Q}{\pi}\ln\left(sh\frac{\pi z}{2h_b}\right) \tag{12}$$

Where z=x+iy. The complex velocity is therefore obtained:

$$W(z) = \frac{dF}{dz} = -\frac{Q}{2h_b}cth\frac{\pi z}{2h_b} \tag{13}$$

Along the streamline vertically below the branch with x=0, we get:

$$W(z) = u - iv = i\cdot\frac{Q}{2h_b}\cot\left(\frac{\pi y}{2h_b}\right) \tag{14}$$

The velocity components are therefore obtained as:

$$\begin{cases} v_x = 0 \\ v_y = \dfrac{Q}{2h_b}\cot\left(\dfrac{\pi y}{2h_b}\right) \end{cases} \tag{15}$$

The gas phase velocity at the wave crest is then determined:

$$v_{y,crest} = \frac{Q}{2h_b}\cot\left(\frac{\pi s}{2h_b}\right) \tag{16}$$

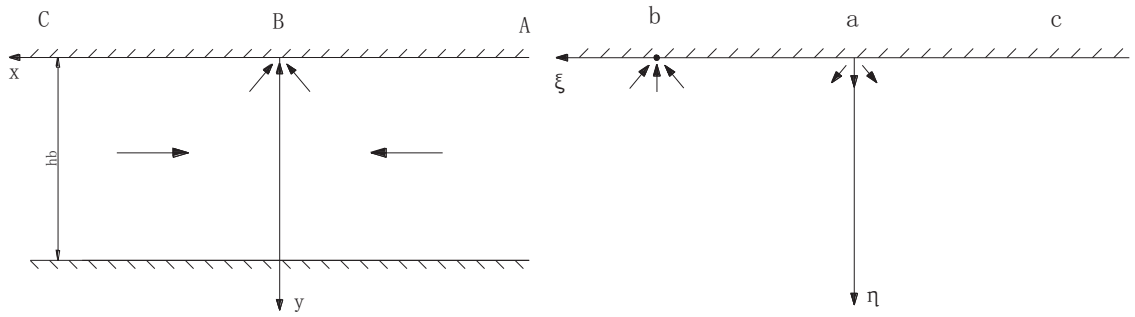

(a) (b)

Figure 10. Schematic of physical and supplementary plane.

The growth rate of liquid column v_f is much smaller than the gas phase velocity v_g when the liquid drop is about to detach from the gas-liquid interface. The entrainment onset criteria is rewritten by substituting the above equation in Eq. 11 and omitting the v_f term:

$$\frac{\pi}{2}C_D\rho_g R^2\frac{Q}{2h_b}\cot^2\left(\frac{\pi s}{2h_b}\right) \geq \sigma\cdot 2\pi R + \rho_f\frac{2}{3}\pi R^3 g \tag{17}$$

The length of the liquid column a is assumed to be proportional to the width of the column λ/2 which is on the order of the branch diameter as observed in the experiment. Under this assumption, the gravity term in Eq. 17 is minor compared with the surface tension term and therefore can be removed from the equation. Additionally, assuming that the vertical distance between the branch inlet and the wave crest s is proportional to the branch diameter d. The Eq. 17 is transformed with some manipulation and expressed as follows:

$$Bo \cdot Fr^2 \geq C_1 \cdot \frac{1}{\pi} \cdot \frac{\rho_f}{\Delta\rho} \cdot \left(\frac{h_b}{d}\right)^3 \cdot \tan^2\left(C_2 \frac{\pi}{2}\left(\frac{h_b}{d}\right)^{-1}\right) \quad \left(0.60 < \frac{h_b}{d} < 1.10\right) \tag{18}$$

The above equation is the entrainment onset semi-empirical correlation and C_1 and C_2 are constants determined by the experimental data. Bo is the bond number measuring the importance of surface tension forces compared to body forces. The best fit to experimental data gives C_1 and C_2 1.56×10^3 and 0.71 respectively. The current model shows good agreement with the experimental data. The average prediction relative error of the model is 43.9%. The prediction error is mainly caused by the high degree of scatter of the test data. The comparison between the current model with different bond numbers and existing models is shown in Figure 11. It can be seen that the current model shows good agreement with the Schrock et al.'s [8] and Smoglie et al.'s [6] correlation in low h_b/d range while showing good agreement with Welter et al.'s and Maciaszek et al.'s correlation in high h_b/d range.

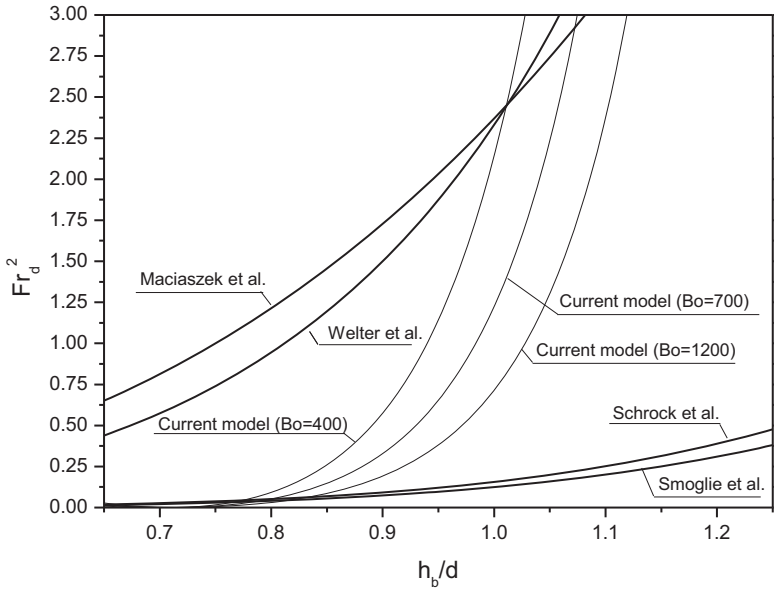

Figure 11. Comparison between the newly developed model and existing models

5. CONCLUSIONS

Entrainment onset and entrainment rate visualization experiments have been conducted with steam-water on ADETEL. Experimental data of entrainment onset and entrainment rate have been acquired and compared with available correlations. A clear difference exists between ADETEL entrainment onset data and available correlations, which may be caused by the differences in physical properties, horizontal pipe flow conditions, methods to determine entrainment onset or d/D ratios. The RELAP5 code may not applicable in the ADS-4 entrainment onset estimation in AP1000 due to the discrepancy between test data and Smoglie et al.'s [6] correlation. The entrainment onset is more likely to be reached in small d/D ratios conditions due to the stronger Bernoulli effects. In this respect, AP1000 has increased safety than AP600

design. The amount of entrained water will drop dramatically with the decreases of liquid level for lower liquid level in the hot leg for a specified steam flow rate.

The upper plenum entrainment experiment has been conducted on modified ADETEL facility with steam-water to validate the reactor safety analysis codes. Tests were conducted without reactor internals installed. The test data shows that the steam flow has little effect on the entrainment under stable experimental conditions. As the mixture liquid level in the pressure vessel decreases, both the entrainment amount and the entrainment amount decreasing rate decline.

The entrainment onset model has been developed based on the experimental data. The effect of surface tension has been taken into consideration in the process of liquid column split. Potential theory and force balance method are introduced in the modeling. The model shows good agreement with the experimental data. The average prediction relative error of the model is 43.9%. The prediction error is mainly caused by the high degree of scatter of the test data.

NOMENCLATURE

A	Wave cross section area
a	Amplitude of wave (m)
Bo	Bond number (-)
C	Constant (-)
d	ADS-4 branch diameter (m)
D	Hot leg diameter (m)
F	Force (N); Complex potential
Fr	Froude number (-)
g	Gravitational acceleration (m/s^2)
h	Height (m)
Q	Volumetric flow rate (m^3/s)
R	Curvature radius of the wave crest (m)
s	Vertical distance between branch inlet and wave crest (m)
v	Velocity (m/s)
W	Complex velocity (-)
w	Mass flow rate (kg/s)
x	Quality (-)
Greek symbols	
λ	Wave space (m)
$\Delta\rho$	Density difference of gas and liquid (kg/m^3)
ρ	Density (kg/m^3)
σ	Surface tension (N/m)
Subscripts	
3	ADS-4 branch line
b	Beginning of entrainment (Entrainment onset)
D	Drag force
d	Branch
g	Steam; Gravity
f	Liquid
y, crest	Y position of the wave crest
σ	Surface tension

ACKNOWLEDGMENTS

The authors would like to express their thanks to the State Nuclear Power Technology R&D Center (No. 2011ZX06004-007) for its sponsorship of the ADS-4 entrainment and depressurization experimental program.

REFERENCES

1. Lin, C.G, *Passive Safety Advanced PWR Nuclear Power Technology (in Chinese)*, Atomic Energy Press, Beijing, (2008).
2. Wang, W.W., Su, G.H., Qiu, S.Z., "Thermal hydraulic phenomena related to small break LOCAs in AP1000," *Progress in Nuclear Energy* **53**, pp. 407-419 (2011).
3. D.C. Sun, S.Z. Qiu, Y. Xiang, "Experimental investigation of liquid entrainment in ADS-4 depressurization line with steam-water," *Experimental Thermal and Fluid Science* **61**, pp. 221-229 (2015).
4. D.C. Sun a, Y. Xiang a, W.X. Tian, Experimental investigation of upper plenum entrainment in AP1000 *Progress in Nuclear Energy* **80,** pp.80-85 (2015).
5. Zuber, N., *Problems in modeling of small break LOCA*, U.S. Nuclear Regulatory Commission, NUREG-0724, (1980).
6. Smoglie, C., Reimann, J., Muller, U., "Two-phase flow through small breaks in a horizontal pipe with stratified flow," *Nucl. Eng. Des*. **99**, pp. 117-130 (1987).
7. The RELAP5 Code Development Team, *RELAP5/MOD3 Code Manual*, U.S. Nuclear Regulatory Commission, (1995).
8. Schrock, V.E., Revankar, S.T., Mannheimer, R., *Small break critical discharge: The roles of vapor and liquid entrainment in a stratified two-phase region upstream of the break*. U.S. Nuclear Regulatory Commission, NUREG/CR-4761, LBL-2204, (1986)
9. Maciaszek, T., Micaelli, J.C., "CATHARE phase separation modeling for small breaks in horizontal pipes with stratified flow," *Nucl. Eng. Des.* **124**, pp. 247-256 (1990).
10. Welter, K.B., Wu, Q., You, Y., "Experimental investigation and theoretical modeling of liquid entrainment in a horizontal tee with a vertical-up branch," *Int. J. Multiphase Flow* **30**, pp. 1451-1484 (2004).
11. Sun, D.C., Zhang, J., Xiang, Y., "Experimental investigation of liquid entrainment in vertical up tee branch with double-end gas inlets," *Ann. Nucl. Eng.* **76**, pp. 315-322 (2015).
12. Kataoka, I., Ishii, M., "Mechanistic modeling of pool entrainment phenomenon," *Int. J. Heat. Mass Transf.* **27** (11), pp. 1999-2014 (1984).
13. Kim, C.H., No, H.C., "Liquid entrainment and off-take through the break at the top of a vessel," *Nucl. Eng. Des.* **235**, pp. 1675-1685 (2005).
14. Wu, Qiao, Young, E.P., Abel, K., Yao, Y., Yoo, Yeon-Jong, "Liquid entrainment in reactor vessel," *Proceedings of 13rd International Conference on Nuclear Engineering*, Beijing, China (2005).
15. Welter, K.B., Bajorek, S.M., *APEX-AP1000 confirmatory testing to support ap1000 design certification*. U.S. Nuclear Regulatory Commission, NUREG -1826, (2005).
16. Sun, D.C., Tian, W.X., Qiu, S.Z., "Scaling analysis of AP1000 ADS-4 entrainment and depressurization," *Progress in Nuclear Energy* **74**, pp.71-78 (2014).
17. D.C. Sun, Y. Xiang, J. Zhang, "Experimental investigation of liquid entrainment in AP1000 ADS-4 branch line with air-water," *Experimental Thermal and Fluid Science* **57**, pp 317-323 (2014).
18. The RELAP5 Code Development Team, *RELAP5/MOD3 Code Manual*. U.S. Nuclear Regulatory Commission, (1995).
19. Mingyuan Zhang, *Advanced Engineering Fluid Mechanics*, Xi'an Jiaotong University Press, Xi'an, (2006).